

DIRECT DETERMINATION OF THE TOTAL WIDTH OF THE η' MESON USING THE COSY-11 APPARATUS*

ERYK CZERWIŃSKI

on behalf of the COSY-11 Collaboration

M. Smoluchowski Institute of Physics, Jagiellonian University
Reymonta 4, 30-059 Kraków, Poland

and

Institute for Nuclear Physics and Jülich Center for Hadron Physics
Research Center Jülich, 52425 Jülich, Germany

(Received February 9, 2009)

We describe the experimental method and consecutive steps of the analysis of the $pp \rightarrow pp\eta'$ reaction measured by means of the COSY-11 detection setup. The conducted investigation aim at the determination of the total width of the η' meson directly from its mass distribution. The preliminary results show that the statistical error is in the order of ≈ 10 keV.

PACS numbers: 13.75.Cs, 14.40.Aq

1. Introduction

Inputs for the phenomenological description of Quantum Chromodynamics in the non-perturbative regime [1] can be provided from studies of the η' meson production [2] and its decays [3]. Such investigations are of interest on its own account and are planned to be conducted with WASA-at-COSY [4], KLOE-2 [5] and CBall-at-MAMI [6] experiments. In addition, precise determinations of the partial widths for the η' decay channels will be helpful for the development of the Chiral Perturbation Theory as constrains for the calculations. However, regardless of the branching ratios of the η' meson decays which are typically known with an accuracy better than 1.5%, the total width is established about 10 times less accurate [7] and cause that the experimental precision of the partial width for various decay channels — where only the branching ratio is known or will be measured — is governed by the precision in the knowledge of the total width.

* Presented at the Symposium on Meson Physics, Kraków, Poland, October 1–4, 2008.

In the last issue of the *Review of Particle Physics* a value of (0.205 ± 0.015) MeV/ c^2 is given for the total width of the η' meson ($\Gamma_{\eta'}$) resulting from a fit which includes a combination of partial widths obtained from integrated cross-sections and branching ratios from 50 measurements [7].

This indirect determination introduces correlation between the value of the $\Gamma_{\eta'}$ and the branching ratios making difficulties in the investigations of the other properties of the η' meson [8].

On the other hand, the mean value from the only two direct measurements [9,10] taken into account by PDG amounts to (0.30 ± 0.09) MeV/ c^2 [7] and differs from the fit result for $\Gamma_{\eta'}$.

Therefore, a precise determination of the natural width of the η' meson may have a large impact on the physics results which will be derived from measurements at facilities like COSY, DAΦNE-2 and MAMI-C and may solve the discrepancy in the values from the direct measurements and the indirect determination which is recommended as the nominal width.

This situation encouraged us to conduct investigations of $\Gamma_{\eta'}$ directly from the missing mass distribution of the $pp \rightarrow pp\eta'$ reaction measured near the kinematical threshold. The advantage of a study close to the threshold is that the uncertainties of the missing mass determination are considerably reduced since at threshold the value of $\partial(\text{mm})/\partial p$ approach zero (mm = missing mass, p = momentum of the outgoing protons).

2. Experiment

In September and October 2006 data of the $pp \rightarrow ppX$ reaction were collected using the COSY-11 detection setup [11], a hydrogen cluster target [12] and the stochastically cooled proton beam of COSY [13]. Five beam momenta: 3211, 3213, 3214, 3218 and 3224 MeV/ c (corresponding to the excess energy of 0.9, 1.5, 1.8, 3.1 and 5.0 MeV, respectively) were used. The collision of a proton from the COSY beam with a cluster target proton may cause an η' meson creation. The ejected protons of the $pp \rightarrow pp\eta'$ reaction were separated from the circulating beam by the magnetic field due to their lower momenta and were registered by the detection system consisting of drift chambers and scintillation counters as depicted in Fig. 1 (top). The reconstruction of the momentum vector for each registered particle is based on the measurement of the track direction by means of the drift chambers, the knowledge of the dipole magnetic field and the target position. Together with the independent determination of the particle velocity from the measured time of flight between the S1 and S3 scintillators the particle identification is provided. The knowledge of the momenta of both protons before and after the reaction allows to calculate the mass of a not observed particle or system of particles in the outgoing channel, which in case of the $pp \rightarrow pp\eta'$ reaction should be equal to the mass of the η' meson.

In order to improve the experimental resolution of the four-momentum determination and in order to decrease the momentum spread of the beam protons reacting with the target two major changes have been applied to the COSY-11 setup (Fig. 1) with respect to the previous measurements of the $pp \rightarrow pp\eta'$ reactions [14–16]. Namely, the spatial resolution of the drift chambers was improved by increasing the supply voltage up to the maximum allowed value and also the width of the target in the direction perpendicular to the COSY beam was decreased from 9 to *circa* 1 mm [12, 17].

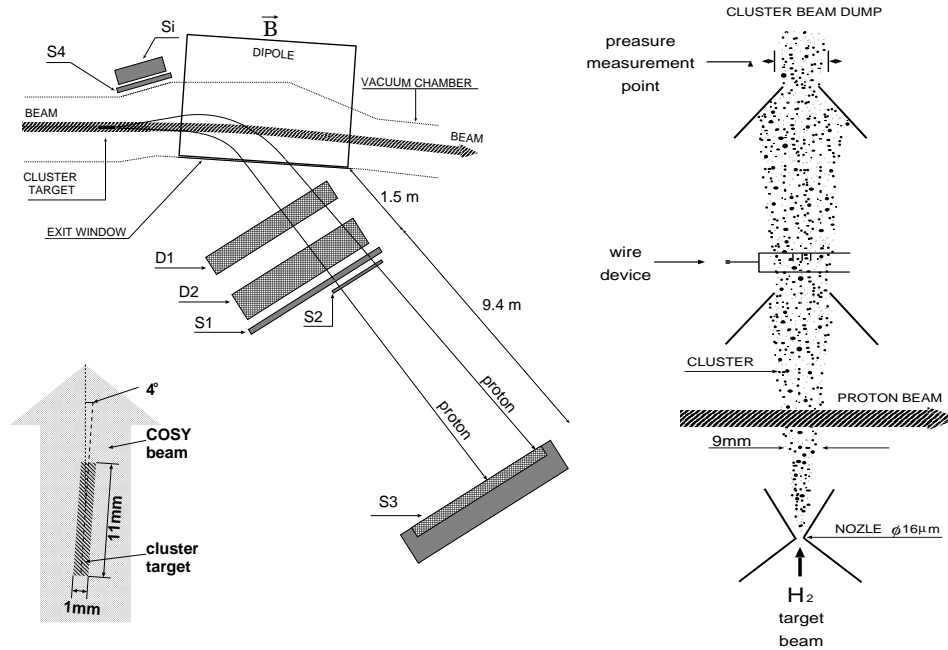


Fig. 1. Left: Top view at the COSY-11 detection setup with drift chambers (D1, D2) used for the reconstruction of trajectories of positively charged ejectiles and scintillator hodoscopes (S1, S2, S3) for the time of flight determination. The silicon pad (Si) and scintillator (S4) detectors register the elastically scattered protons used for monitoring purposes. Right: Schematic side view of the target and beam crossing. The diagnosis unit for the target dimensions measurement installed above the reaction region does not influence the $pp \rightarrow pp\eta'$ measurement. Bottom Left: Cross-section of the cluster target stream in the COSY beam plane.

2.1. Detectors

The trajectory of a charged particle passing through the drift chambers (DC) is obtained from the dependency between drift time of the electrons (from the gas ionized by that particle) going towards the sense wire and the

distance between sense wire and particle trajectory. The evaluation of this dependency is based on the assumption that the particle trajectory inside the drift chamber is a straight line. The drift time to distance relation was calibrated for each 20–24 hours of the data taking period in order to minimise fluctuations of the drift velocity caused by variations of atmospheric pressure, air humidity and gas mixture changes. Fig. 2 (upper left) illustrates that the obtained spatial resolution equals to about $100 \mu\text{m}$.

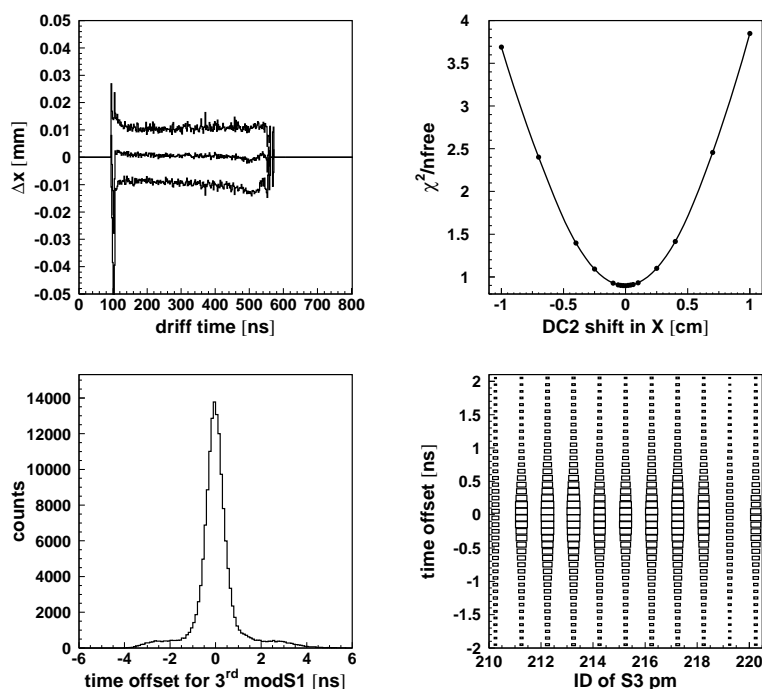


Fig. 2. Top left: Average deviation (ΔX) between the measured and the fitted distances of tracks from the sense wire as a function of the drift time. The histogram around 0 corresponds to the average value of the ΔX distribution and the upper and lower lines denotes the standard deviation of the ΔX distribution. Top right: χ^2 distribution for the fit of the straight line to the signals from both drift chambers as a function of the position of the second with respect to the first drift chamber. Bottom: Distributions of difference between the time-of-flight measured using S1–S3 detectors and the time-of-flight calculated from the momentum reconstructed based on the curvature of the trajectory in the magnetic field. As an example spectra for 3rd S1 module and a range of photomultipliers (pm) of S3 detector are shown. The counting rate of PM 210 and 219 is smaller since these photomultipliers are positioned at the edges of the detector.

The velocity of the charged particle is measured by means of the S1(S2) and S3 scintillator detectors applying the time of flight (ToF) method. For the calibration of the scintillator detectors we compare the time-of-flight obtained from signals registered in the S1 and S3 detectors and the time-of-flight calculated from the reconstructed momentum of the particle. As an example the lower plots in Fig. 2 present results of the calibration for arbitrarily chosen photomultipliers (pm) of the S1 and S3 detectors.

In order to correct a possible misalignment of the drift chambers after 10 years of operation in the COSY ring a sample of events with a single tracks was used, and the relative position of chambers was established as these corresponding to the minimum in the χ^2 distribution of the fit made under the assumption of a straight trajectory of a particle through both DCs (Fig. 2 upper right). The absolute position of both DCs was established utilising the shape of the kinematical ellipse of the elastically scattered protons (Fig. 3).

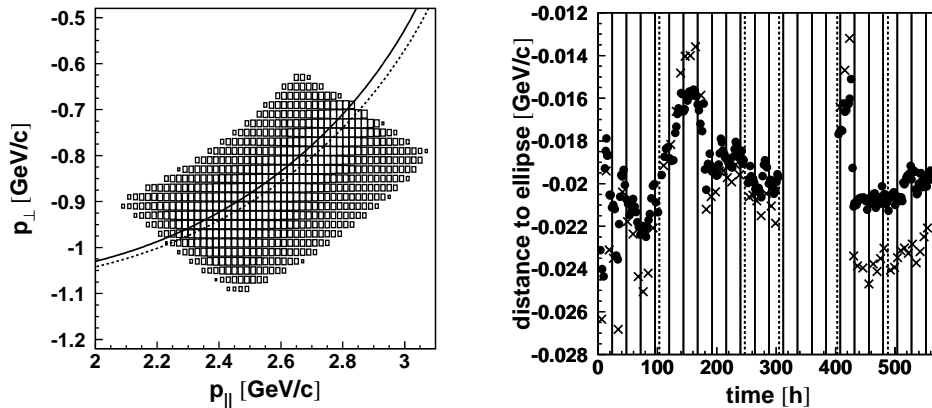


Fig. 3. Left: Part of the kinematical ellipse of elastically scattered protons collected at a nominal beam momentum of 3211 MeV/c. The solid line denotes the position of the ellipse for the real beam momentum of 3211 MeV/c. The dashed line shows the centre of the reconstructed ellipse which corresponds to a beam momentum of 3250 MeV/c. Right: Distance of the reconstructed kinematical ellipse of the elastically scattered protons to the nominal (expected) one as a function of time of the measurement. The straight lines mark 24 hour intervals. The dashed lines separate the different beam momenta (3218, 3211, 3214, 3213 and 3224 MeV/c). Filled circles include events with a signal in the first S1 module, crosses for events with signals in the 4th module. The events in the range from 0–300 h were used for the absolute position determination of the drift chambers.

2.2. Target

The intersection of COSY beam and cluster target stream defines the reaction region. The centre of that volume is always assumed as origin for the reconstruction of the trajectory of protons ejected from any point in this region. Therefore in order to decrease the reconstructed momentum spread one needs to decrease the reaction region. Such decrease additionally lowers the momentum spread of the proton beam overlapping with the target due to the dispersion in the target area in front of the dipole magnet.

For the experiment described in this report the size of the target stream was reduced by inserting an appropriately shaped aperture. For the precise monitoring of the size of the target stream in the interaction region a diagnosis unit with wires rotating through the cluster target beam was installed, see Fig. 1. When moving the wires through the cluster target beam the pressure in that region was changed and from the pressure profile the target size and position could be determined, see Fig. 4. As a cross-check the size of the interaction region was monitored also based on the shape of the kinematical ellipse of the elastically scattered protons applying the method described in article [18].

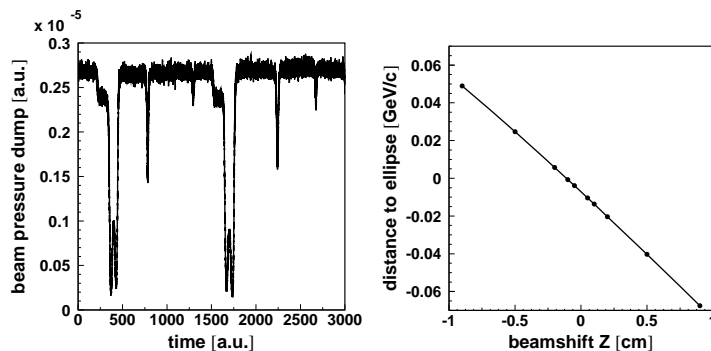


Fig. 4. Left: Profile of the pressure measured during the wire device rotation. The observed structures depend on the position and size of the cluster target stream. Right: (MC) Distance of the reconstructed kinematical ellipse of the elastically scattered protons to the nominal (expected) one as a function of the relative position of the target beam. The observed deviation for a non-shifted target are due to the different procedures used during generation and reconstruction of events.

Several measurements with the diagnosis unit and the continuous registration of the $pp \rightarrow pp$ reaction allow to check the stability of the target stream as a function of time. Small fluctuations on a large time scale were observed (Fig. 3). Such fluctuations cannot be due to variations of the COSY beam momentum because they would require an unrealistic momentum change ten times larger than the typical uncertainty in the COSY

settings. Any variations of the target position in the X direction perpendicular to the proton beam would be in contradiction to the information from the diagnosis unit. The only reasonable solution to explain the fluctuation is a shift of the reaction area in Z direction (longitudinal to the proton beam) by ≈ 1 mm (Fig. 4 right). This variations of the position of the kinematical ellipse can be explained by fluctuations of the density inside the target stream.

The observed phenomenon has a big influence on the achieved missing mass spectra as is seen from a comparison of distributions obtained for first and second half of the measurement at the beam momentum of 3211 MeV/ c (see Fig. 5).

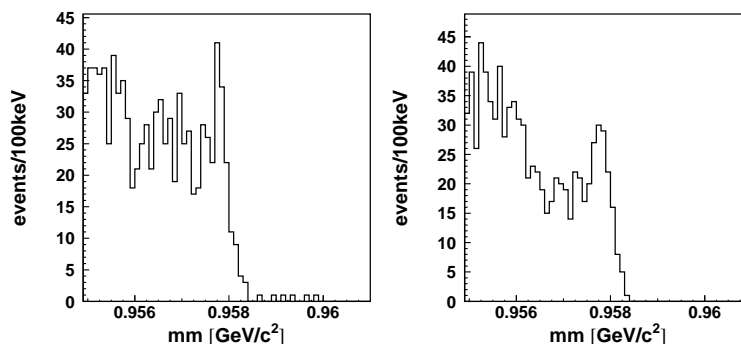


Fig. 5. Missing mass distribution for the $pp \rightarrow ppX$ reaction for the first (left) and the second (right) half of the measurement at beam momentum of 3211 MeV/ c .

3. Results

As an example Fig. 6 presents one out of five missing mass spectra obtained from the experiment. The present results were obtained without taking into account the density variations inside the target.

For each beam momentum a set of Monte Carlo histograms for different assumed total width of the η' meson was prepared. The extraction of the value of $\Gamma_{\eta'}$ and of its statistical error rests on the simultaneous comparison of all five experimental missing mass spectra with distributions simulated for a given value of $\Gamma_{\eta'}$. The normalisation factors were the only free parameters in the fit. A preliminary result of the χ^2 dependence on the $\Gamma_{\eta'}$ is shown in Fig. 7. The achieved statistical error in the determination of $\Gamma_{\eta'}$ is equal to about 10 keV. At present the absolute value of the width is under evaluation and it will be reported after correcting for fluctuations of the distribution of the target density.

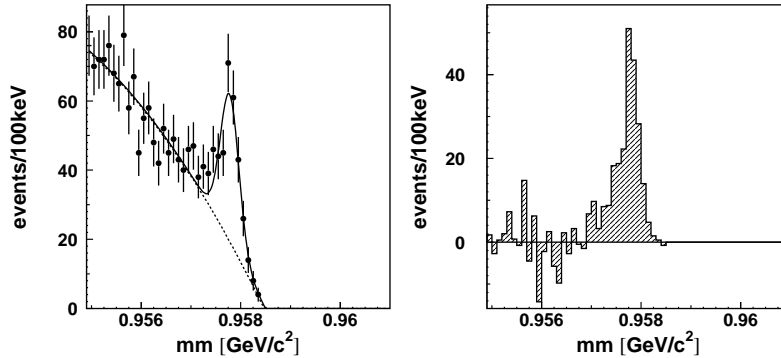


Fig. 6. Preliminary missing mass spectra with background (left) and background-corrected (right) for 3211 MeV/c beam momentum. A 2nd order polynomial was used for the background description. For the further analysis a normalised background from a signal-free range in spectra from other beam momenta will be used. For details see [19].

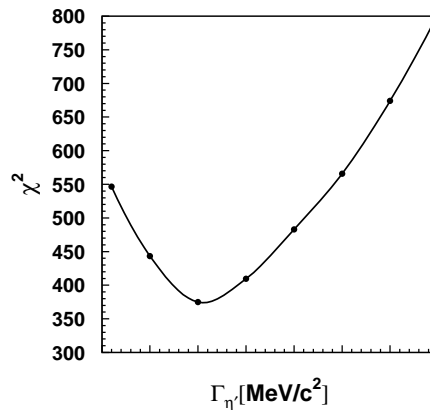


Fig. 7. χ^2 dependence on the $\Gamma_{\eta'}$ obtained from the comparison of the experimental and simulated missing mass spectra. For the calculation a Poisson likelihood χ^2 was used as derived from the maximum likelihood method [20, 21].

The work was supported by the European Community Research Infrastructure Activity under the FP6 program (Hadron Physics, RII3-CT-2004-506078), by the German Research Foundation (DFG), by the Polish Ministry of Science and Higher Education through grants No. 3240/H03/2006/31 and 1202/DFG/2007/03, and by the FFE grants from the Research Center Jülich.

REFERENCES

- [1] B. Borasoy, R. Nissler, *AIP Conf. Proc.* **950**, 180 (2007).
- [2] P. Moskal, [hep-ph/0408162](#).
- [3] A. Kupść, *AIP Conf. Proc.* **950**, 165 (2007).
- [4] H.-H. Adam *et al.*, [nucl-ex/0411038](#).
- [5] F. Ambrosino *et al.*, *Eur. Phys. J.* **C50**, 729 (2007).
- [6] A. Thomas, *AIP Conf. Proc.*, **950**, 198 (2007).
- [7] C. Amsler *et al.* [Particle Data Group], *Phys. Lett.* **B667**, 1 (2008).
- [8] B. Di Micco, *Acta Phys. Pol. B Proc. Suppl.* **2**, 63 (2009), these proceedings.
- [9] D.M. Binnie *et al.*, *Phys. Lett.* **B83**, 141 (1979).
- [10] R. Wurzinger *et al.*, *Phys. Lett.* **B374**, 283 (1996).
- [11] S. Brauksiepe *et al.*, *Nucl. Instrum. Methods* **A376**, 397 (1996).
- [12] H. Dombrowski *et al.*, *Nucl. Instrum. Methods* **A386**, 228 (1997).
- [13] D. Prasuhn *et al.*, *Nucl. Instrum. Methods* **A441**, 167 (2000).
- [14] P. Moskal *et al.*, *Phys. Rev. Lett.* **80**, 3202 (1998).
- [15] P. Moskal *et al.*, *Phys. Lett.* **B474**, 416 (2000).
- [16] A. Khoukaz *et al.*, *Eur. Phys. J.* **A20**, 345 (2004).
- [17] A. Täschner *et al.*, *AIP Conf. Proc.* **950**, 85 (2007).
- [18] P. Moskal *et al.*, *Nucl. Instrum. Methods* **A446**, 448 (2001).
- [19] P. Moskal *et al.*, *J. Phys. G* **32**, 629 (2006).
- [20] S. Baker, R.D. Cousins, *Nucl. Instrum. Methods* **221**, 437 (1984).
- [21] G.J. Feldman, R.D. Cousins, *Phys. Rev.* **D57**, 3873 (1998).